Biochemistry and Biophysics Reports 18 (2019) 100624

Contents lists available at ScienceDirect

Biochemistry and Biophysics Reports

journal homepage: www.elsevier.com/locate/bbrep

E0771 and 4T1 murine breast cancer cells and interleukin 6 alter gene expression patterns but do not induce browning in cultured white adipocytes

Janina V. Pearce[a,b], Jared S. Farrar[a,b], Joseph C. Lownik[a], Bin Ni[b], Shanshan Chen[b,c], Tiffany W. Kan[b,d], Francesco S. Celi[b,*]

[a] Center for Clinical and Translational Research, Virginia Commonwealth University School of Medicine, Richmond, VA, USA
[b] Department of Internal Medicine, Division of Endocrinology, Diabetes and Metabolism, Virginia Commonwealth University School of Medicine, Richmond, VA, USA
[c] Department of Biostatistics, Virginia Commonwealth University School of Medicine, Richmond, VA, USA
[d] Rollins School of Public Health, Emory University, Atlanta, GA, USA

ARTICLE INFO

Keywords:
E0771 breast cancer
4T1 breast cancer
Interleukin 6
Adipose tissue
White adipose tissue browning
Uncoupling protein 1

ABSTRACT

Breast cancer remains a substantial clinical problem worldwide, and cancer-associated cachexia is a condition associated with poor prognosis in this and other malignancies. Adipose tissue is involved in the development and progression of cancer-associated cachexia, but its various roles and mechanisms of action are not completely defined, especially as it relates to breast cancer. Interleukin 6 has been implicated in several mechanisms contributing to increased breast cancer tumorigenesis, as well as a net-negative energy balance and cancer-associated cachexia via adipose tissue remodeling in other models of cancer; however, its potential role in breast cancer-associated white adipose browning has not been explored. In this study, we demonstrate localized white adipose tissue browning in a spontaneous model of murine mammary cancer. We then used an *in vitro* murine adipocyte culture system with the E0771 and 4T1 cell lines as models of breast cancer. We demonstrate that while the E0771 and 4T1 secretomes and cross-talk with white adipocytes alter white adipocyte mRNA expression, they do not directly induce white adipocyte browning. Additionally, we show that neither exogenous administration of interleukin 6 alone or with its soluble receptor directly induce white adipocyte browning. Together, these results demonstrate that neither the E0771 or 4T1 murine breast cancer cell lines, nor interleukin 6, directly cause browning of cultured white adipocytes. This suggests that their roles in adipose tissue remodeling are more complex and indirect in nature.

1. Introduction

Breast cancer is the most common cancer diagnosed in the majority of countries worldwide and is a leading cause of cancer death [1]. Cancer-associated cachexia (CAC) is a condition common to virtually all types of malignancies, including breast cancer [2], and is characterized by the loss of skeletal muscle mass with or without the loss of adipose tissue mass. CAC is a multifaceted condition and is a predictor of poor prognosis, implicated in an estimated 20% of cancer-related deaths [3,4]. Recent experimental observations indicate that adipose tissue remodeling plays an important role in the development and progression of CAC (reviewed by Ref. [5]).

While white adipose tissue (WAT) functions as a source of energy storage, thermogenic adipose tissue – classically brown adipose tissue (BAT), but also “beige” and “brown-in-white” adipose tissue [6,7] – functions in the opposite manner, utilizing energy instead of storing it [8]. This unique function of thermogenic fat is attributable largely to the presence and action of uncoupling protein 1 (UCP1), which results in an increase in substrate utilization and heat production. Maladaptive thermogenic adipose tissue expansion and activity in response to cancer have been implicated as a potential contributor to CAC (reviewed by Ref. [5]).

Interleukin 6 (IL6), an inflammatory cytokine with pleiotropic actions, has various roles in the breast and tumor environment, which includes cancer cells and adipocytes as well as adipocyte precursors, endothelial cells, and macrophages [9]. Elevated IL6 levels increase protein catabolism and skeletal muscle wasting which contributes to CAC [10]. Through its canonical signaling pathway via signal transducer and activator of transcription 3 (STAT3), the role of IL6 in CAC has been expanded to include other organ systems beyond skeletal

Abbreviations: CAC, cancer-associated cachexia; WAT, white adipose tissue; BAT, brown adipose tissue; IL6, interleukin 6; UCP1, uncoupling protein 1

* Corresponding author. 1101 East Marshall Street 7-007, Richmond, VA, 23298, USA.
E-mail address: francesco.celi@vcuhealth.org (F.S. Celi).

https://doi.org/10.1016/j.bbrep.2019.100624
Received 11 December 2018; Received in revised form 20 February 2019; Accepted 5 March 2019
Available online 20 March 2019

muscle, including adipose tissue (reviewed by Ref. [11]). IL6 is thought to be involved in the dedifferentiation and inflammatory characteristics of breast cancer-associated adipocytes [12] and has been shown to stimulate WAT lipolysis [13]; however, its roles in BAT activation and WAT browning are only of recent interest. Increased BAT activity and WAT browning occurs in cancer and may contribute to CAC [14–16]. Specifically, IL6 has been implicated as a direct driver of WAT browning in models of colon cancer [13,15].

While these studies have demonstrated the presence of WAT browning in several models of cancer, the roles of breast cancer itself and of IL6 in breast cancer-related WAT browning have not been explored. Breast cancer represents an ideal experimental model to investigate the mechanisms by which maladaptive WAT browning may occur, due to its anatomic contiguity with breast adipose tissue. In this study, we explored whether WAT browning occurs in murine breast cancer, and sought to answer if E0771 or 4T1 cells, well-characterized murine breast cancer cell lines, or IL6 are potential drivers of WAT browning in an *in vitro* cell culture system. Our results highlight the importance of studying WAT browning in different cancer models to provide insight into various drivers of this process, with the goal of developing therapeutic strategies to attenuate CAC in patients with cancer.

2. Materials and methods

Mice were bred and maintained in animal facilities under standard housing conditions and utilized in accordance with protocols approved by the Institutional Animal Care and Use Committee (IACUC) at Virginia Commonwealth University. All materials were purchased from Sigma-Aldrich unless noted otherwise.

2.1. Histology and immunohistochemistry

B6·FVB-Tg (MMTV-PyVT)634Mul/LellJ mice (Jackson Laboratory) were raised in animal facilities under standard housing conditions. These mice develop palpable tumors after, on average, 3 months (92 days) of life, and at later timepoints can develop lung metastases. Bilateral adipose tissue pads (interscapular BAT, axillary WAT, inguinal WAT, and ovarian WAT), with tumor when applicable, were harvested from female mice at approximately 4 months of age (approximately 121 days), to ensure all axillary and inguinal mammary pads had palpable tumors. Tissues were immediately placed into 10% buffered formalin (Fisher Chemical) for 6 days, and then transferred to 70% ethanol until embedding and sectioning was performed by the VCU Massey Cancer Center Cancer Mouse Model Shared Resource. All tissues were processed via a Sakura Tissue Tek automated processor using a standard dehydration, clearing, and paraffin infiltration program, and were sectioned at 5 μm thickness.

Mouse UCP1 expression in the tissues was detected via immunohistochemistry (IHC) using the SuperPicture 3rd Gen IHC Detection Kit (Invitrogen) and slight protocol modifications in the same batch. Slides were deparaffinized in xylene and rehydrated in a graded series of ethanol, ending with distilled water and finally PBST. Slides were then placed in citrate buffer diluted to 1× in distilled water and heated in a microwave for antigen retrieval. Peroxidase quenching solution (included in kit) was placed on slides and incubated for 10 min. After washing with PBST, slides were covered with 5% BSA (Fisher Scientific, diluted in TBST) for 1 h. The slides were incubated in UCP1 primary antibody (abcam 10983, diluted 1:500 in 1% BSA) at 4 °C in a dark cold room overnight. The next day, after washing with PBST, HRP Polymer Conjugate (included in kit) was added and left to incubate for 30 min. Slides were washed in PBST and DAB Chromogen (included in kit) was added for approximately 2 min to visualize binding. Slides were then washed with tap water and counterstained with diluted Hematoxylin Solution Gill No.2 for 30 s. After washing with tap water, slides were dehydrated using a reverse-graded series of ethanol, ending with xylene, and glass slides were mounted using HistoChoice Mounting Media (Amresco/VWR).

Slides were digitally scanned using the NanoZoomer 2.0-HT Whole Slide Imager Digital Pathology Slide Scanner (Meyer Instruments) by the Department of Pathology.

2.2. MATLAB analysis of IHC images

All IHC images were captured using the same magnification and processed and analyzed in MATLAB 2017a. A customized algorithm was developed to automatically detect and quantify the number of brown pixels in every vertical column within the region of interest for each IHC image. The region of interest was defined as the adipose tissue without tumor using the following criteria: horizontal borders – top and bottom edges of the image; vertical borders – vertical column(s) closest to, but not including, tumor, then extending distally to left and/or right edges of the image. The counts were plotted against the column index (which indicates the distance to the tumor cells, or horizontal distance from tumor) for curve fitting.

2.3. Stromal vascular fraction isolation, culture, and differentiation

Primary isolation of inguinal stromal vascular fraction (SVF) cells from female C57BL/6 J or BALB/cJ wild-type mice (both from Jackson Laboratory) aged 22–25 days was performed using established protocol [17]. Isolated SVF cells were grown in a basal cell culture medium consisting of DMEM/F-12 + Glutamax (Thermo Fisher) supplemented with 10% Fetal Bovine Serum (FBS, Thermo Fisher), 200U/mL penicillin, 0.2 mg/mL streptomycin, 25 μg/mL amphotericin B, and 100 μg/mL Normocin (InvivoGen). Cells were plated on cell culture plates coated with 0.1% gelatin solution according to manufacturer protocol and grown to confluency in basal cell culture medium before differentiation. For white adipocyte differentiation, an induction cocktail comprised of basal medium without Normocin supplemented with 5 μg/mL insulin, 1 μM dexamethasone, 0.5 mM 3-isobutyl-1-methylxanthine (IBMX), and 125 μM indomethacin was used for 4 days. After induction, differentiating white adipocytes were cultured in a maintenance cocktail comprised of basal medium without Normocin supplemented with 5 μg/mL insulin for 12 days. For beige adipocyte differentiation, induction cocktail comprised of basal medium without Normocin supplemented with 5 μg/mL insulin, 5 μM dexamethasone, 0.5 mM IBMX, 125 μM indomethacin, 0.5 μM rosiglitazone, and 1 nM triiodothyronine (T3) and was used for 4 days. After induction, differentiating beige adipocytes were cultured in a maintenance cocktail comprised of basal medium without Normocin supplemented with 5 μg/mL insulin, 1 μM rosiglitazone, and 1 nM T3 for 12 days. See next subsections for experimental conditions after maturation. Medium for all cells was changed every 2–3 days. The maximum passage number used for any primary SVF experiments was passage 4.

2.4. Cancer cell culture, conditioned medium, and coculture experiments

E0771 cells (CH3 BioSystems) and 4T1 cells (ATCC CRL-2539) were grown in basal cell culture medium comprised of RPMI1640 + GlutaMAX (Thermo Fisher) supplemented with 10% FBS and 200U/mL penicillin, 0.2 mg/mL streptomycin, and 25 μg/mL amphotericin B.

For conditioned medium collection, cells were grown to ~70% confluency, and then cell culture medium was changed. This conditioned medium was harvested 24 h later and filtered through a 0.22 μm pore size filter (Millipore) for use in experiments. For coculture experiments, cancer cells were grown to ~70% confluency on coculture inserts (Fisher Scientific) and then moved to the appropriate adipocyte wells for experiments. Empty coculture wells were placed in all other adipocyte wells. The maximum passage number used for any experiments was passage 11.

Primary SVF cells were isolated, grown, and induced to either

mature white or beige adipocytes as described above. On day 16, mature white adipocytes were exposed to white maintenance medium plus one of the following for 24 h: 1) no treatment (white control), 2) 10 μM CL 316,243 hydrate, 3) cancer conditioned medium in a 1:1 ratio with white maintenance medium cocktail, or 4) cancer coculture. Mature beige adipocytes continued on beige maintenance medium (beige control).

2.5. Interleukin 6 experiments

Mature adipocytes from primary SVF cells were prepared as described above. On day 16, mature white adipocytes were exposed to white maintenance medium plus one of the following for both 30 min and 3 day experiments: 1) no treatment (white control), 2) 10 μM CL 316,243, 3) 40 ng/mL mouse recombinant IL6 (R&D Systems), 4) 40 ng/mL mouse recombinant IL6 + 200 ng/mL mouse recombinant IL6RA (R&D Systems). Mature beige adipocytes continued on beige maintenance medium (beige control).

2.6. Oil Red O staining

Oil Red O was used to stain mature white and beige adipocytes after differentiation according to established Lonza protocol (#WEB-PR-PT-2501 OIL-3). Wells were kept covered with water until visualized by bright-field microscopy using a Zeiss AxioObserver A1 Microscope at the VCU Department of Anatomy and Neurobiology Microscopy Facility.

2.7. RNA isolation and quantification, cDNA generation, and quantitative Real-Time PCR

Total RNA was isolated with TRIzol (Thermo Fisher) according to manufacturer protocol with UltraPure Glycogen (Thermo Fisher). RNA was quantified using the NanoDrop 1000 Spectrophotometer (Thermo Fisher). cDNA was generated using the BioRad iScript cDNA Synthesis Kit (BioRad) with an input of 1 μg RNA on a C1000 Thermal Cycler (BioRad). The cDNA was then diluted 1:3 in molecular grade water.

qPCR was performed on the QuantStudio 3 Real-Time PCR System (Applied Biosystems) with 10 μL per reaction on 96 well plates in technical duplicates or triplicates containing the following: 1× PowerUp SYBR Green Master Mix (Applied Biosystems), 0.5 μM forward and reverse primers (Supplementary Table 1, all purchased from Eurofins Genomics), and 3 μL of cDNA. The Thermo Fisher Cloud platform was used for analysis of efficiency-corrected Cq values using *Tbp* as a reference gene for normalization, and fold-changes ($2^{\Delta\Delta Cq}$) were calculated using Microsoft Excel.

2.8. Protein isolation, quantification, and western blotting

Protein isolation and quantification were performed using RIPA lysis and extraction buffer (Thermo Scientific) and the Pierce BCA Protein Assay Kit (Thermo Scientific) according to manufacturer's 'microplate' protocol. Absorbance was measured at 562 nm using a VersaMax microplate reader (Molecular Devices). A standard curve was generated using a four-parameter curve with SoftMax Pro 5.3 software and was used to determine the protein concentration of experimental samples.

Protein lysates were separated on NuPAGE 4–12% Bis-Tris Midi Gels (Invitrogen) with an input of 20 μg of protein per well using an XCell4 Surelock Midi-Cell (Invitrogen). Gel transfer was performed using the iBlot Transfer Stack, PVDF, regular size (Invitrogen) according to manufacturer's 'dry blot transfer' method. Membranes were further processed using established protocols, with primary and secondary antibody information provided in Supplementary Table 2. Western blot signal was detected using chemiluminescence substrates (Cell Signaling) and images were captured using the ChemiDoc MP Imaging System (BioRad). Stat1/2/3/5 Control Cell Extracts (Cell Signaling) were used for phosphorylated STAT3 negative and positive controls.

2.9. Flow cytometry

Cell surface flow cytometry staining was performed as described previously [18]. Primary SVF cells were isolated, grown, and induced to either mature white or beige adipocytes as described above until day 16. Cells were washed in 1× PBS supplemented with 5% FBS, 2 mM EDTA, and 0.05% sodium azide, then stained for respective targets (Supplementary Table 2) before gentle scraping to remove cells from wells and moved to suspension. Cells were fixed (BioLegend) as single cell suspensions prior to flow cytometry analysis.

For intracellular cytokine flow cytometry, E0771 and 4T1 cells were cultured until ~70% confluent, and murine peritoneal cavity cells (consisting of a variety of immune cells [19]) were isolated by lavage the day preceding each experiment. All cell groups were treated with 1× Brefeldin A (BioLegend), 1× Monensin (BioLegend), 1× phorbol 12-myristate-13-acetate (PMA) and 1× Ionomycin (Thermo Fisher) for 3 h before harvest. Single-cell suspensions were created, stained with live-dead stain (BioLegend), and then incubated with 2.4g2 [20] to block Fc receptors. After fixation, cells were permeabilized using Intracellular Staining Perm Wash Buffer (BioLegend) and then stained for targets (Supplementary Table 2).

Data for both cell-surface and intracellular flow cytometry were acquired on the LSR Fortessa flow cytometer (BD Biosciences) in the VCU Flow Cytometry Core.

Data were analyzed using FCS Express 5 (De Novo Software).

2.10. Statistical analyses

GraphPad Prism was used for visualization of data and statistical analyses. Specific tests used are described in each figure legend. For all analyses and figures, error bars represent standard deviation and p-values are represented as: × $p < 0.05$, ** $p < 0.01$, *** $p < 0.001$, **** $p < 0.0001$. For p-values $0.05 < p < 0.1$, the p-value is included in the appropriate figure area. No annotation indicates a p-value > 0.1 for that comparison.

3. Results and discussion

3.1. White adipose tissue adjacent to murine mammary tumors exhibits features of WAT browning

We first asked whether WAT browning could be observed in a murine model of breast cancer. Adipocytes closest to the tumor-adipocyte interface *in vivo* have increased UCP1 protein expression, the hallmark of thermogenic adipose tissue function (Fig. 1). Compared to their respective ovarian WAT (top left image in Fig. 1, and Supplementary Fig. 1), adipocytes surrounding spontaneous mammary tumors in both axillary and inguinal mammary fat pads demonstrate an increased staining intensity for UCP1 protein (Supplementary Fig. 2), but not as much as their respective interscapular BAT (bottom left image in Fig. 1, and Supplementary Fig. 1). MATLAB analyses were performed on the images with tumor to quantify the number of brown pixels, as a measure of UCP1 staining intensity, across each image, with representative results shown in Fig. 1. The increase in UCP1 protein expression is most robust at the tumor-adipose tissue interface, and UCP1 protein expression sharply declines moving further from the tumor, demonstrated by a trend that fits the inverse power law upon curve fitting (bottom right image in Fig. 1). This suggests that the strength of browning is inversely related to the center of its driver, the tumor cells, which has recently been noted in a xenograft model of breast cancer as well [21]. We also observe smaller lipid droplets in these adipocytes, which has been observed and described as a characteristic of 'cancer-associated adipocytes (CAA)' at the tumor forefront

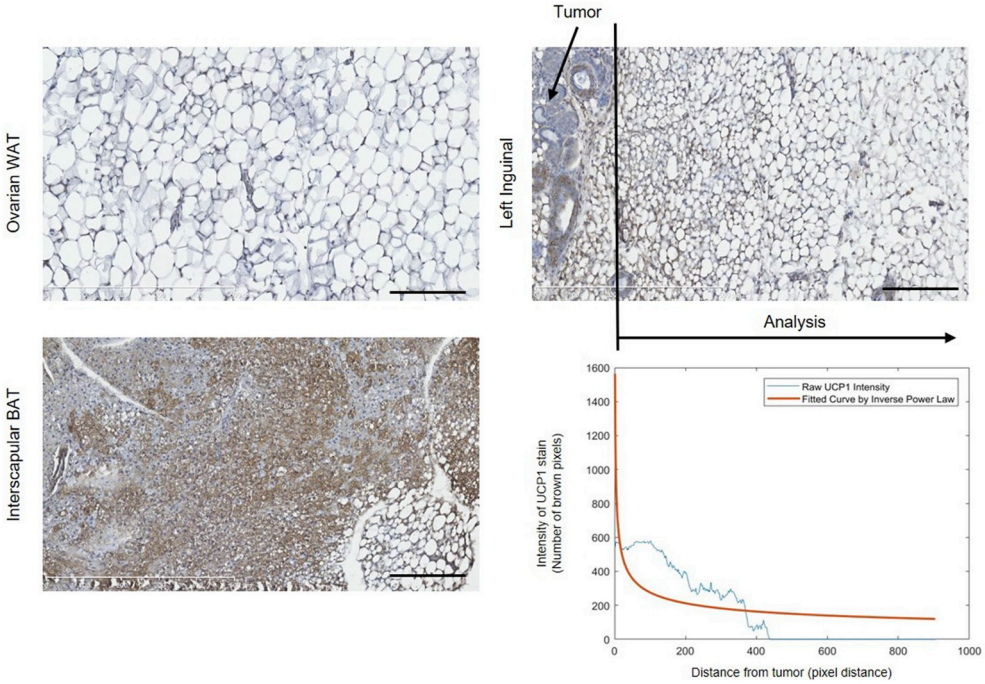

Fig. 1. Immunohistochemistry shows increased UCP1 protein expression in adipocytes adjacent to spontaneous mammary tumors. Representative images from four-month old female MMTV-PyVT mouse tissue harvested and stained for UCP1 protein. Ovarian WAT = negative control, interscapular BAT = positive control. Inguinal mammary fat pad with tumor was analyzed via MATLAB (bottom right), indicating a sharp decline in UCP1 staining intensity with increasing distance from the tumor. Scale bars = 200μm. UCP1 = uncoupling protein 1, WAT = white adipose tissue, BAT = brown adipose tissue.

[22]. Together, the decreased lipid size and increased UCP1 expression in adipocytes closest to the tumor in our IHC images confirm the phenotypic changes consistent with a maladaptive transdifferentiation from white to beige adipose tissue in response to the tumor microenvironment. Furthermore, the localized nature of this browning suggests a paracrine signaling interaction between the tumor and adjacent adipocytes.

3.2. Differentiation of white and beige adipocytes from primary stromal vascular fraction cells provides a robust in vitro model to detect adipocyte browning

Based on the extremely localized WAT browning observed *in vivo*, we established a cell culture system which would allow us to methodically and systematically study the effects of individual components of the tumor microenvironment on adipocytes *in vitro*. Several murine cell lines are used for adipogenesis studies *in vitro*, such as the 3T3-L1 cell line [23] or immortalized SVF cells [24]. However, the use of a non-immortalized primary SVF cell system using female mice is important for studying the effects of breast cancer on adipocyte browning. We demonstrate that primary SVF cells (also referred to as preadipocytes) are capable of undergoing differentiation to both mature white and beige adipocytes (Fig. 2). Oil Red O staining demonstrates successful differentiation in both white and beige groups, with larger lipid droplets in the white differentiation group (Fig. 2A). Expression of *Dlk1* (Delta like non-canonical Notch ligand 1, also known as *Pref-1*), a marker of immature/undifferentiated adipocytes, is appropriately elevated in undifferentiated preadipocytes compared to differentiated white and beige adipocytes (Fig. 2B). Expression of white adipocyte-associated genes *Cfd* (complement factor D, also known as adipsin) and *Lep* (leptin) were significantly lower in both preadipocytes (not expressed for leptin) and beige adipocytes relative to white adipocytes, and expression of *Fasn* (fatty-acid synthase) was significantly lower in preadipocytes (Fig. 2C). Lastly, expression of thermogenic adipocyte genes *Cidea* (cell death-inducing DNA fragmentation factor, alpha subunit-like effector A), *Ppargc1a* (peroxisome proliferative activated receptor, gamma, coactivator 1 alpha), *Tnfrsf9* (tumor necrosis factor receptor superfamily, member 9), and *Ucp1* were significantly increased in differentiated beige adipocytes (Fig. 2D). Although there are many genes associated with thermogenic adipocytes, *Ucp1* is the hallmark for thermogenic activity, and the other three genes – *Cidea*, *Ppargc1a*, and *Tnfrsf9* – were selected because of their established use throughout the literature as key markers to help identify thermogenic adipocytes [25–27].

Together, these *in vitro* gene expression profiles are appropriate when compared to those of other models and whole tissue lysates [26]. Additionally, the exposure of white differentiated adipocytes to CL 316,243, a β3 adrenergic agonist used as a positive control, results in an appropriate increase in *Ucp1* mRNA expression (for example, Fig. 3A). This unique feature provides a model of white to beige adipocyte transdifferentiation. Together, these data demonstrate that the differentiation of primary inguinal SVF cells from female mice provides a robust cell culture system, which is uniquely suited for studying the local effects of breast cancer and other components within the tumor microenvironment on adipocyte browning.

3.3. E0771 and 4T1 conditioned medium and coculture alter white adipocyte mRNA expression but do not induce browning in differentiated white adipocytes

After establishing our *in vitro* cell culture system, we first asked whether breast cancer cells themselves can induce localized WAT browning as observed *in vivo*. E0771, an estrogen-receptor positive murine breast cancer cell line on the C57BL/6 background, is commonly used in many *in vitro* and *in vivo* C57BL/6 breast cancer studies [28–31]. The 4T1 breast cancer cell line is an animal model for stage IV breast cancer, has a more metastatic phenotype than E0771 cells [32], and is commonly used for *in vitro* and *in vivo* BALB/c breast cancer studies [33] and allograft studies [34,35]. Use of these established breast cancer cell lines, as opposed to the use of whole tumor lysate, provides a strategic advantage in the mechanistic study of WAT browning *in vitro* because they are cultured without other cells within the tumor microenvironment, which could confound results, and eliminates the problems of inter- and intra-organism tumor heterogeneity [36,37].

We first utilized our *in vitro* cell culture system to explore whether the E0771 cell secretome or E0771 coculture with white adipocytes would induce WAT browning by measuring *Ucp1* mRNA, as UCP1 is the

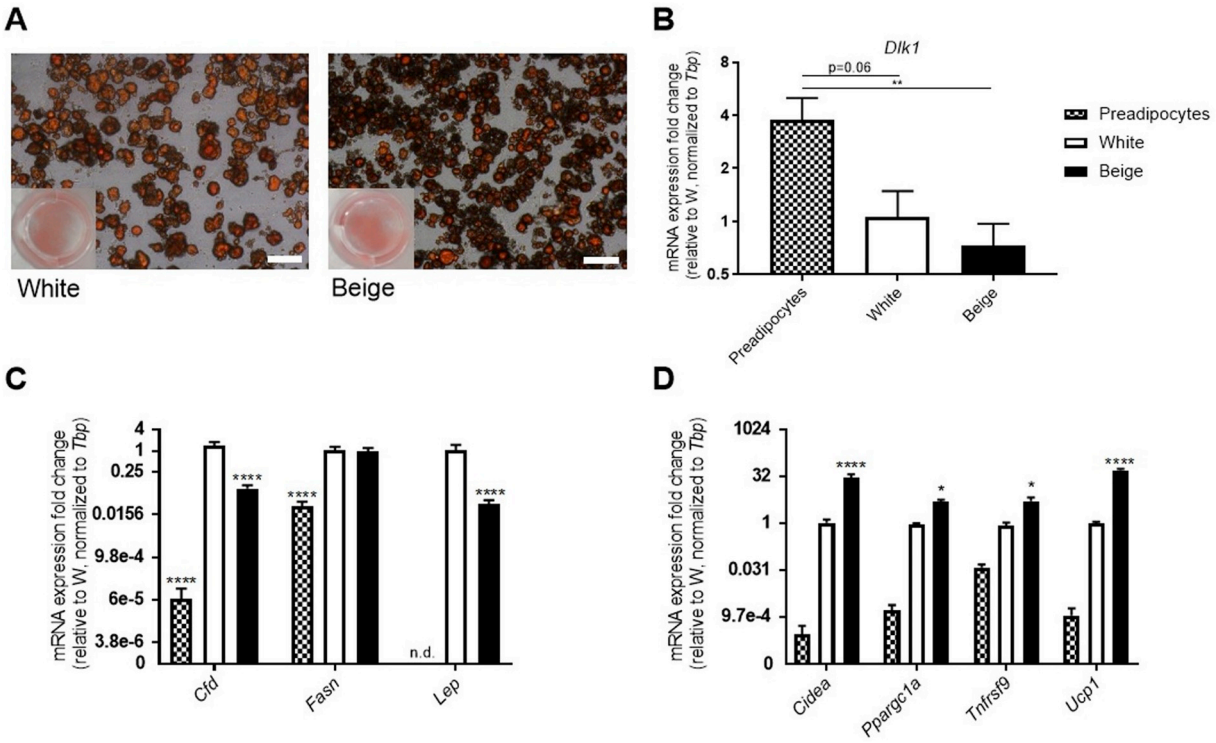

Fig. 2. Primary SVF cells are capable of differentiation to mature white and beige adipocytes. Inguinal SVF cells isolated from young female C57BL/6 J mice were differentiated to either white or beige adipocytes as described in methods. (A) Representative Oil Red O staining confirming that our protocol is highly selective for culture of preadipocytes capable of undergoing successful differentiation. Scale bars = 100 μm. Quantitative PCR for (B) *Dlk1*, a marker for undifferentiated preadipocytes, (C) markers of white adipocytes, and (D) markers of thermogenic adipocytes. Please note y-axis scale is log2. n = 5 primary SVF cell lines. Statistical tests: (B) Kruskal-Wallis and Dunn's multiple comparisons tests, (C) and (D) Two-way ANOVA and Dunnett's multiple comparisons tests. SVF = stromal vascular fraction, n.d. = not detected.

hallmark protein of thermogenic adipose tissue activity. We exposed differentiated, mature white adipocytes to the conditioned medium from E0771 murine breast cancer cells (Fig. 3), or cocultured them with E0771 cells (Fig. 4). To our surprise, *Ucp1* mRNA expression in white adipocytes exposed to both treatment groups was *decreased* relative to control white adipocytes, and was significantly decreased when compared to both control beige adipocytes and white adipocytes exposed to the β3 adrenergic agonist CL 316,243 (Figs. 3A and 4A). Although not statistically significant, the trend of lower *Ucp1* expression in white adipocytes exposed to either the E0771 secretome or E0771 coculture was opposite our original expectations. Western blotting of UCP1 confirmed these mRNA expression results on the protein level (Fig. 3E).

While there were no changes in gene expression of the thermogenesis-associated genes *Cidea* or *Ppargc1a*, white adipocytes cocultured with E0771 cells expressed significantly more *Tnfrsf9* (Fig. 4B). White adipocytes exposed to conditioned medium had increased, although not statistically significant, *Tnfrsf9* (Fig. 3B). *Tnfrsf9* has been found to be elevated in breast cancer xenografts [21], but within adipocytes, its expression changes often parallel *Ucp1* and *Ppargc1a* [38], which we did not observe in our results. TNFRSF9 (also known as CD137) promotes the activation of a variety of immune cells [39], and can enhance natural killer cell-mediated destruction of breast cancer cells [40]. It is therefore possible that cross-talk between white adipocytes and the E0771 cell line induces an immune-eliciting/enhancing response by the adipocytes.

Lep and *Fasn* mRNA levels were significantly decreased in both treatment conditions compared to control differentiated white adipocytes, with no change in *Cfd* expression (Figs. 3C and 4C). In adipocytes, leptin expression usually increases in cases of nutrient excess, so it was initially surprising that its expression is decreased in our experimental system with plentiful nutrients in the cell culture medium. However, leptin is overexpressed in breast tumors [41] and contributes to tumorigenesis by playing a role in mesenchymal-epithelial transition and in regulating angiogenesis [42]. Therefore, we suspect that the observed decrease in *Lep* expression by mature white adipocytes represents a protective response after exposure to E0771 conditioned medium or coculture. Multiple studies have shown that overexpression of fatty acid synthase, a key enzyme for *de novo* fatty acid synthesis, in breast cancer cells confers a more aggressive phenotype and allows for tumor growth and migration [43], so its decreased expression in adipocytes after treatment is consistent with a protective response. Additionally, transcription of *Fasn* is regulated, at least in part, by leptin [44], whose mRNA expression we show here as also being downregulated.

We also tested for genes associated with lipolysis, and found that white adipocytes exposed to E0771 cancer-conditioned medium had no changes in expression of *Lpl* (lipoprotein lipase) or *Mgll* (monoglyceride lipase), but expressed less *Lipe* (hormone sensitive lipase) compared to control white adipocytes (Fig. 3D). However, expression of *Mgll* was significantly increased in white adipocytes cocultured with E0771 cells, while expression of *Lipe* and *Lpl* was decreased but not significantly (Fig. 4D). Increased monoglyceride lipase, an enzyme involved in lipolysis to generate fatty acids, is implicated in progression of several cancer cell types, including aggressive breast cancer [45]. Our results suggest that E0771-adipcyte cross talk, not simply E0771 cell secretome components, may induce *Mgll* expression to provide substrates for E0771 cancer cell utilization.

Lastly, we repeated these experiments using white adipocytes from BALB/cJ SVF and the 4T1 breast cancer cell line. 4T1 conditioned medium exposure or coculture with BALB/c-derived mature adipocytes demonstrated very similar results to our E0771 experiments. *Ucp1* mRNA expression in white adipocytes exposed to 4T1 cancer conditioned medium or 4T1 coculture was *decreased* relative to control white adipocytes, although not statistically significant (Supplementary

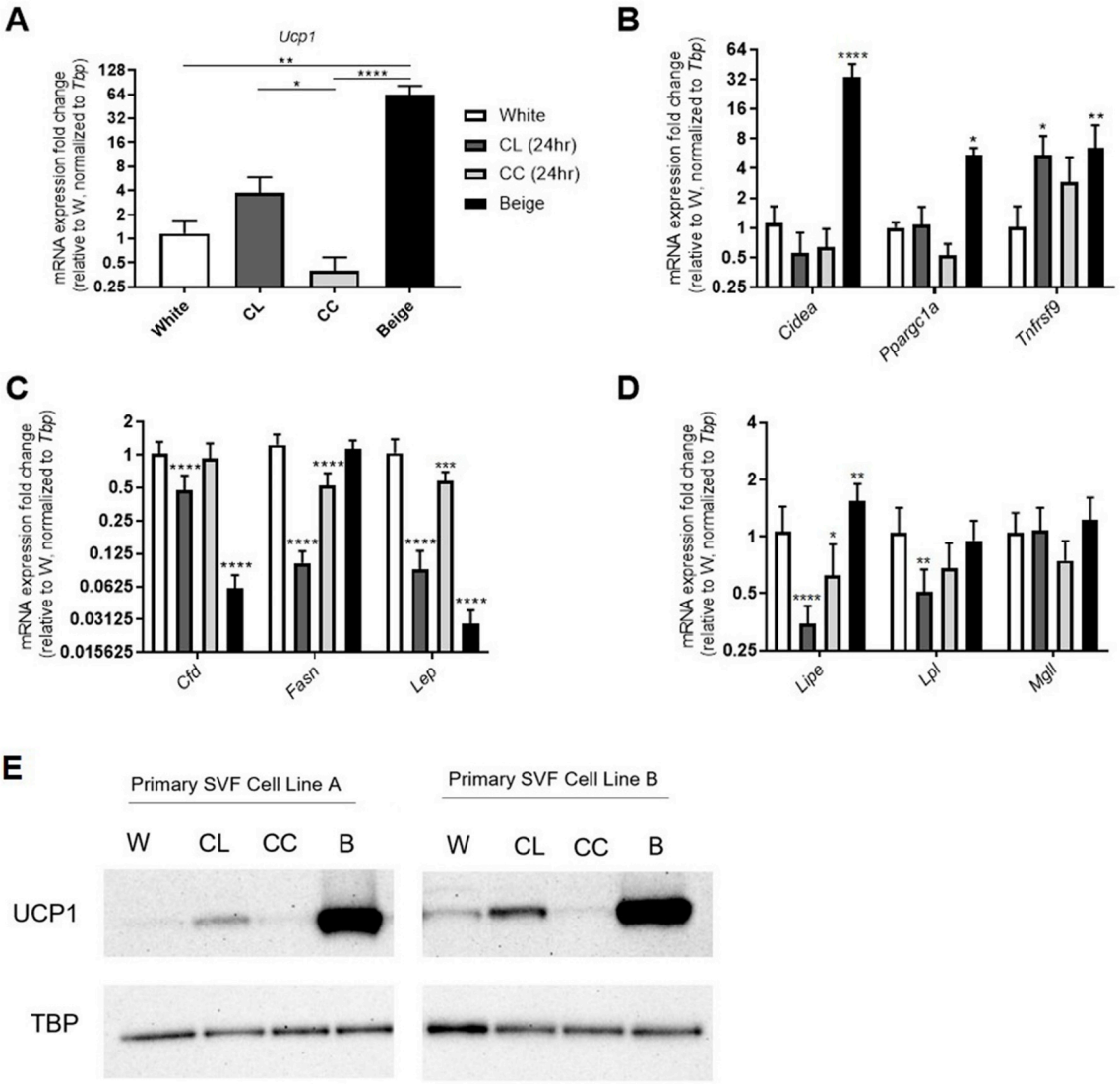

Fig. 3. E0771 cancer-conditioned medium alters white adipocyte mRNA expression, but does not induce white adipocyte browning *in vitro*. Differentiated white adipocytes from C57BL/6 J SVF were treated with CL 316,243 (noted as 'CL' in images) or cancer-conditioned medium (noted as 'CC' in images) and compared to controls as described in methods. Quantitative PCR for (A) *Ucp1*, (B) other markers of thermogenic adipocytes, (C) markers of white adipocytes, and (D) markers of lipolysis. Please note y-axis scale is log2. N = 7 primary SVF cell lines. (E) Representative western blot of UCP1 and TBP in two of the primary SVF cell lines used in this experiment, furthering supporting that E0771 cancer-conditioned medium does not induce white adipocyte browning *in vitro*. Statistical tests: (A) Kruskal-Wallis and Dunn's multiple comparisons tests, (B), (C), and (D) Two-way ANOVA and Dunnett's multiple comparisons tests.

Fig. 3A and Supplementary Fig. 4A, respectively). There were no statistically significant changes in thermogenic adipocyte-related gene expression, although there was a trend towards increased *Tnfrsf9*. As described above, it is still possible that an immune-eliciting/enhancing response by the adipocytes occurs in the presence of breast cancer. The only white adipocyte gene marker that was changed in these 4T1 experiments was a decrease in *Lep* expression after exposure to 4T1 cancer conditioned medium (Supplementary Fig. 3C). This is slightly different from the E0771 results, which demonstrated a decrease in *Lep* and *Fasn* in both treatment groups, but still suggests that a decrease in *Lep* expression by mature white adipocytes represents a protective response in the presence of breast cancer. No changes in any of the lipolysis-related genes occurred in the 4T1 experiments, which suggests that differences between the E0771 and 4T1 cancer cell lines and/or C57BL/6- and BALB/c-derived adipocytes may influence this aspect of adipocyte plasticity.

Together, our results show that E0771 and 4T1 conditioned medium and coculture modify the overall adipocyte gene expression pattern, but do not alter thermogenic gene expression. This supports prior literature regarding non-thermogenic changes in cancer, and challenges those related to cancer-induced WAT browning; however, since the *in vivo* environment is multifaceted, the complexities of the cells and signaling within the tumor microenvironment should be explored further before completely ruling out WAT browning effects from these murine breast cancer cell lines.

3.4. Exposure of differentiated white adipocytes to exogenous IL6 does not increase Ucp1 gene expression, but alters white adipocyte mRNA expression

Since tumor-derived IL6 has been directly implicated in other models of cancer-related WAT browning [15], we asked whether it possesses the ability of generating white to brown transdifferentiation in our primary adipocyte cell culture system. We first investigated whether the E0771 or 4T1 cells secrete IL6 into the conditioned medium. Cells were treated with PMA and ionomycin, which overstimulate cytokine production, as well as brefeldin A and monensin,

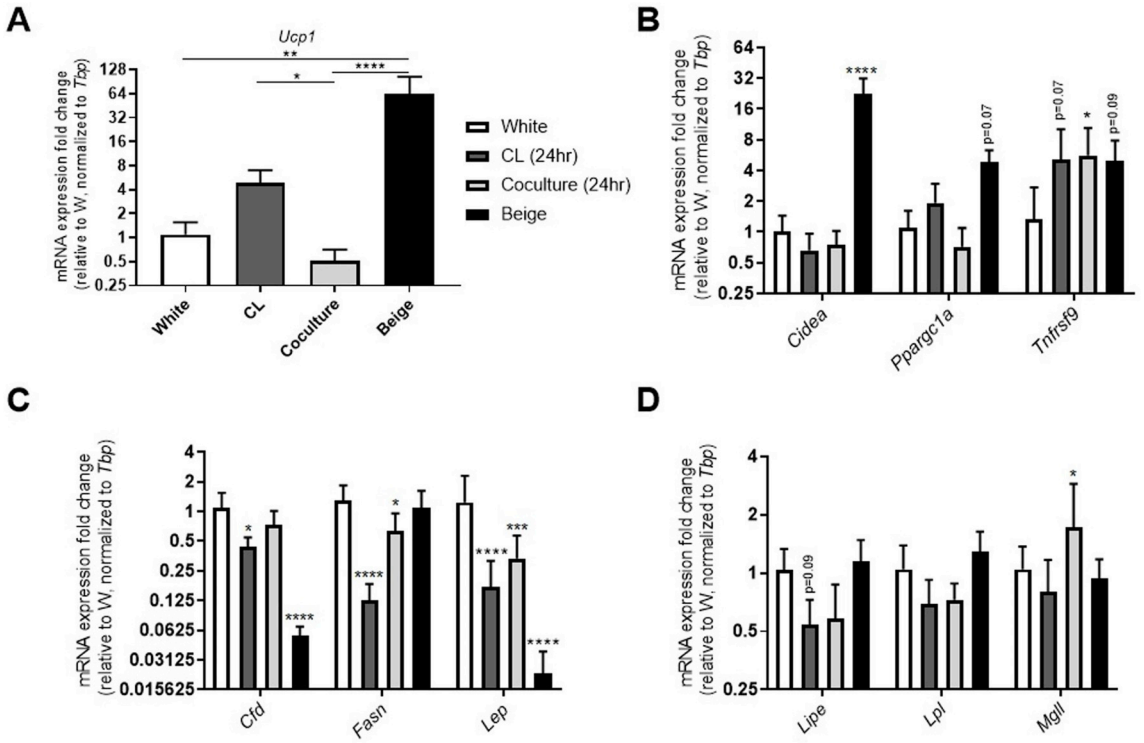

Fig. 4. E0771 coculture alters white adipocyte mRNA expression, but does not induce white adipocyte browning *in vitro*. Differentiated white adipocytes from C57BL/6 J SVF were treated with CL 316,243 (noted as 'CL' in images) or cocultured with E0771 cells (noted as 'Coculture' in images) and compared to controls as described in methods. Quantitative PCR for (A) *Ucp1*, (B) other markers of thermogenic adipocytes, (C) markers of white adipocytes, and (D) markers of lipolysis. Please note y-axis scale is log2. N = 7 primary SVF cell lines. Statistical tests: (A) Kruskal-Wallis and Dunn's multiple comparisons tests, (B), (C), and (D) Two-way ANOVA and Dunnett's multiple comparisons tests.

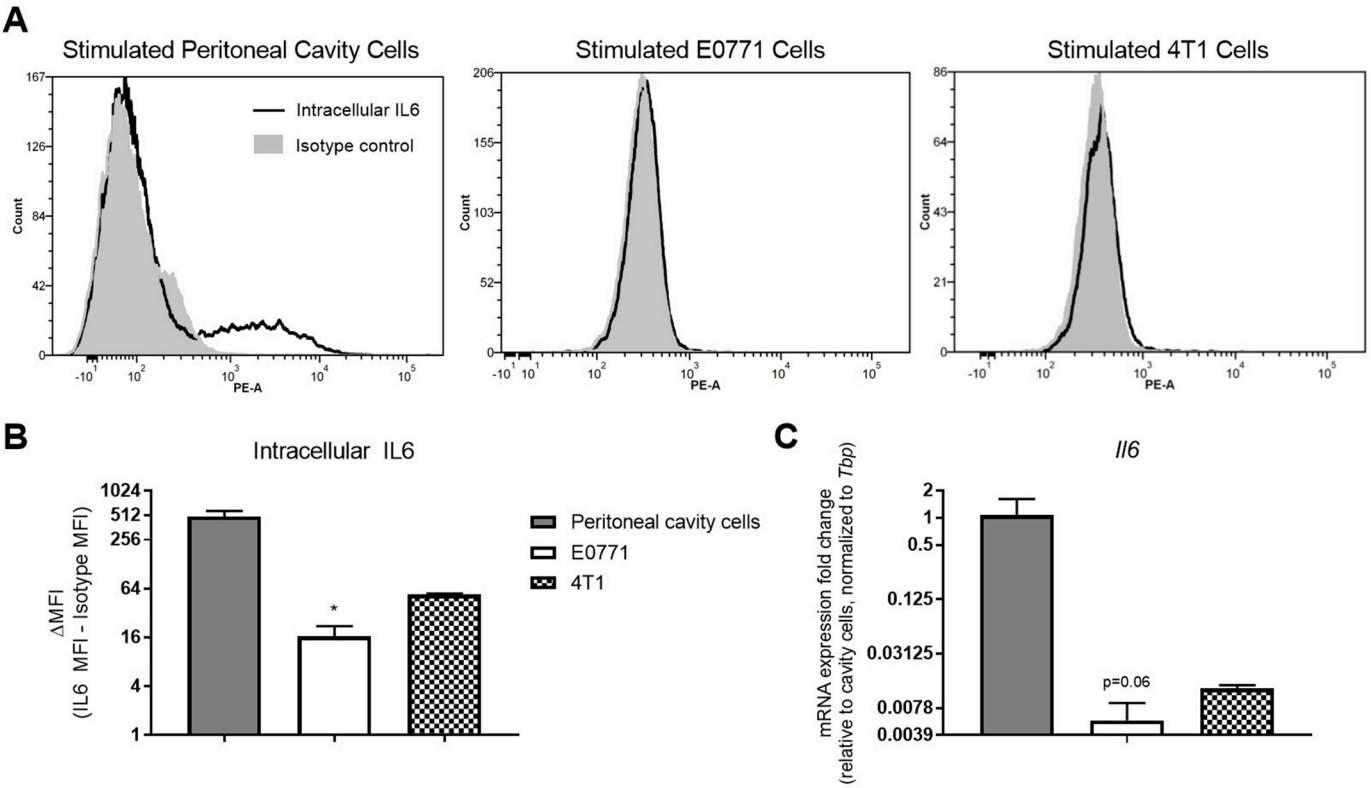

Fig. 5. E0771 and 4T1 murine breast cancer cells do not produce excessive IL6. Peritoneal cavity, E0771, and 4T1 cells were stimulated to induce endogenous IL6 production as described in methods. (A) Intracellular flow cytometry curves showing staining data for IL6 stain and isotype control. (B) Quantification of intracellular IL6 from flow cytometry MFIs. (C) Quantitative PCR for *Il6* mRNA expression. Please note y-axis scale in (B) and (C) is log2. N = 2 for peritoneal cavity cells; n = 3 for E0771 and 4T1 cells. Statistical tests: (B) and (C) Kruskal-Wallis tests for multiple comparisons. MFI = Mean Fluorescent Intensity.

which act to inhibit intracellular protein and trap proteins in the endoplasmic reticulum. This method allowed us to make comparisons in *maximum* IL6 production of each cell type.

Compared with stimulated murine peritoneal cavity cells which contain inflammatory cells, stimulated E0771 cells produce significantly less IL6 when measured by intracellular flow cytometry (Fig. 5A–B) and express over 100-fold less *Il6* mRNA (Fig. 5C). Stimulated 4T1 cells produce less IL6 than peritoneal cavity cells as measured by both flow cytometry (Fig. 5A–B) and qPCR (Fig. 5C), although the results were not statistically significant. Expression and secretion of IL6 directly by breast cancer cells is variable, depending heavily on breast cancer cell type [46,47]. Moreover, it is well established that IL6 is physiologically produced by non-adipocyte cells within adipose tissues [48], and can be modulated by breast adipose tissue in models of breast cancer [49]. Based on this information, we decided to explore whether IL6 would be capable of directly inducing WAT browning, regardless of its cell origin.

As IL6 may come from a variety of cell types within the tumor microenvironment *in vivo* [50–52], we investigated whether our mature adipocytes *in vitro* have the necessary receptor machinery to ensure IL6-mediated signal transduction could occur. IL6 binds to either membrane-bound or soluble interleukin 6 receptor alpha (IL6RA, also referred to as CD126), and this IL6:IL6RA complex then associates with membrane-bound interleukin 6 signal transducer IL6ST (IL6ST, also referred to as GP130 or CD130) to induce signal transduction via the JAK/STAT3 pathway [53]. IL6ST expression is virtually ubiquitous, while expression of membrane-bound IL6RA is more cell-specific [54]. We confirmed that IL6ST is expressed in our mature, differentiated adipocytes, both on the membrane surface as measured by flow cytometry and by transcript levels with qPCR (Fig. 6A–B). Interestingly, flow cytometry data for IL6RA was less than the isotype control, suggesting lack of, or minimal, receptor expression (Fig. 6C). Our expression levels of *IL6ra* mRNA are consistent with this finding; while mRNA was detectable, it was 64- to 128-fold lower than stimulated peritoneal cavity cells (Fig. 6D).

In vivo, soluble IL6RA is produced by breast cancer cells [55] and by monocytes and macrophages [54]; additionally, membrane-bound IL6RA on cells within the tumor microenvironment (such as T-lymphocytes [56]) can be cleaved by shedases such as A Disintegrin And Metalloproteinases (ADAM) family members ADAM10 and ADAM17 to form soluble IL6RA. ADAM10 and ADAM17 have been shown to be upregulated in several tumor models [57,58]. Our results, taken together with this information about the *in vivo* environment, prompted the inclusion of soluble IL6RA in our IL6 exposure experiments to mimic the tumor microenvironment and to ensure that signal transduction could occur.

With this information, we investigated whether exogenous IL6 exposure, with or without supplemented soluble IL6RA, would induce gene expression changes indicative of WAT browning. We observed an increase in *Socs3* (suppressor of cytokine signaling 3) gene expression (Supplementary Fig. 5A) and STAT3 protein phosphorylation (Supplementary Fig. 5B) following just 30 min of exposure to both IL6 and IL6 + IL6RA, although the effect was most robust in the IL6 + IL6RA group. These results confirm the bioactivity of IL6 and IL6RA via STAT3 signaling in our experimental model. To our surprise, exposure of white adipocytes to IL6 or IL6 + IL6RA for three days did not increase *Ucp1* or *Cidea* mRNA expression but instead resulted in a downward trend in expression (Fig. 7A–B), similar to our observations in cancer conditioned medium and coculture experiments (Fig. 3A–B, 4A-B). The IL6 + IL6RA treated group expressed significantly more *Tnfrsf9* mRNA compared to control white adipocytes but had no changes in *Ppargc1a* expression (Fig. 7B), similar to our coculture results. Together, these

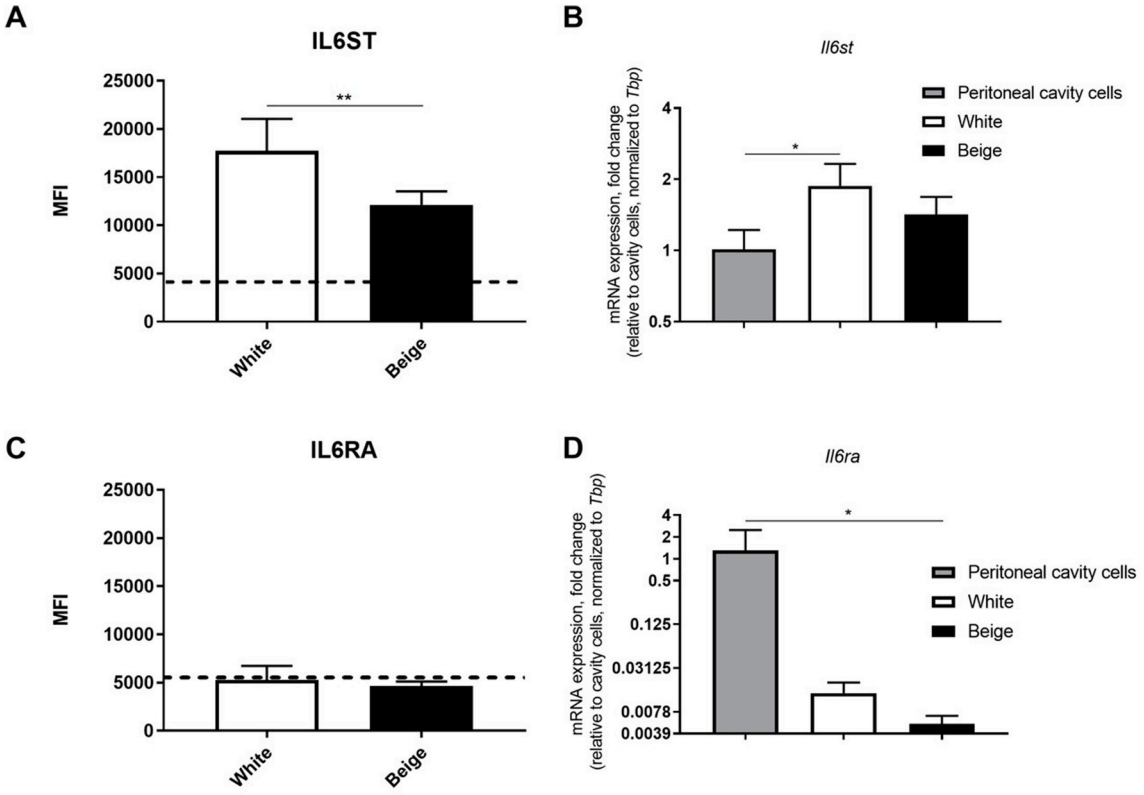

Fig. 6. Differentiated white and beige adipocytes express abundant IL6ST, but not IL6RA. Flow cytometry for (A) cell-surface IL6ST (GP130, CD130) or (C) IL6RA (CD126) in white and beige adipocytes. Dashed line represents average MFI staining for each respective isotype control. Quantitative PCR for (B) *Il6st* (*Gp130*) or (D) *Il6ra* (*Cd126*) for peritoneal cavity cells and white and beige adipocytes. N = 2 for peritoneal cavity cells; n = 5 SVF cell lines for white and beige adipocytes. Please note y-axis scale in (B) and (D) is log2. Statistical tests: (A) and (C) Mann-Whitney test, (B) and (D) Kruskal-Wallis and Dunn's multiple comparisons tests. MFI = Mean Fluorescent Intensity.

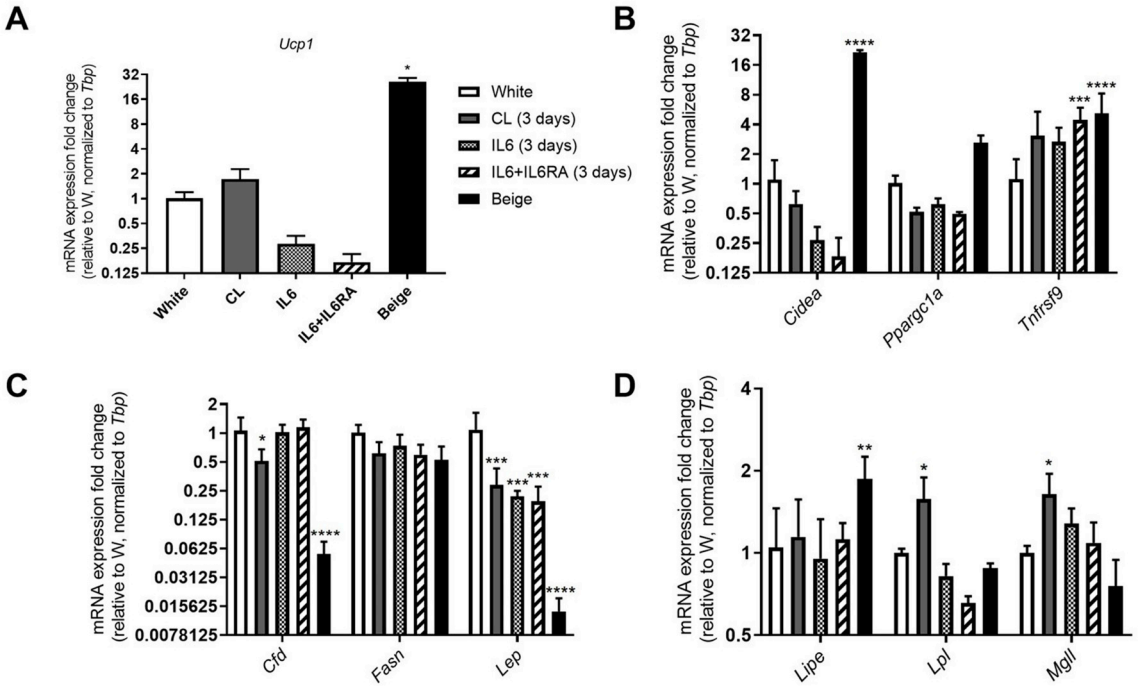

Fig. 7. Neither exogenous IL6 or IL6 + IL6RA administration causes WAT browning *in vitro*. Differentiated white adipocytes from C57BL/6 J SVF were treated for 3 days with CL 316,243 (noted as 'CL' in images), or IL6, or IL6 + IL6RA, and compared to controls as described in methods. Quantitative PCR for (A) *Ucp1*, (B) markers of thermogenic adipocytes, (C) markers of white adipocytes, and (D) markers of lipolysis. Please note y-axis scale is log2. N = 3 primary SVF cell lines. Statistical tests: (A) Kruskal-Wallis and Dunn's multiple comparisons tests, (B), (C), and (D) Two-way ANOVA and Dunnett's multiple comparisons tests.

results suggest that IL6-induced changes to adipocytes *in vivo* may be dependent on soluble receptors from other cells and additional signaling within the tumor microenvironment. *Lep* mRNA expression was significantly decreased with IL6 + IL6RA treatment, similar to our observations in cancer conditioned medium and coculture experiments (Fig. 3A–B, 4A-B), but no changes were observed for *Cfd* or *Fasn* (Fig. 7C). No change in any of the measured lipolysis markers was observed in white adipocytes treated with IL6 + IL6RA (Fig. 7D).

These results, especially the lack of increased *Ucp1* expression, contrast the findings of previous studies that implicate IL6 as a direct causative agent of WAT browning [15]. However, it is important to recognize the differences in our current study and design limitations that may account for these discrepancies. IL6's role in WAT browning was implicated in a model of colon cancer, which is inherently different than breast cancer and the specific cell lines used in our studies. Other molecules, such as parathyroid hormone related peptide, have been implicated in different models of CAC [14], so it is possible that other pathways may be driving the process of WAT browning in breast cancer. Whether IL6 exerts its effects directly or indirectly is still contested within the literature [59], so it is entirely possible that IL6's role in WAT browning in breast cancer may be indirect.

4. Conclusion

In these experiments, we explored whether white adipose tissue browning occurs in a spontaneous model of murine breast cancer *in vivo*, and subsequently investigated the roles of E0771 and 4T1, well-characterized murine breast cancer cell lines, and IL6, a pleotropic cytokine, in an *in vitro* model of WAT browning. We demonstrate that UCP1 expression is locally increased at the tumor-adipose interface *in vivo*, consistent with tumor-induced white to beige adipose tissue transdifferentiation. *In vitro*, our results demonstrate that both E0771 and 4T1 breast cancer cells, as well as IL6 treatment, induce changes to white adipocyte gene expression patterns. However, WAT browning does not occur via direct E0771 or 4T1 cancer cell mechanisms or via direct IL6-mediated STAT3 signaling, pointing to other cell types and/or interactions with cells within the tumor microenvironment as the potential driver of these thermogenic changes. Further investigations are needed to understand the mechanisms behind this process, and to test its impacts on whole body energy expenditure and the development and progression of cancer-associated cachexia.

Declaration of interest

The authors have no conflicts of interest related to this work.

Funding

Services and products in support of the research project were generated by the VCU Massey Cancer Center's Pilot Project Program and the VCU Massey Cancer Center Cancer Mouse Model, Flow Cytometry, and Microscopy Shared Resources, supported, in part, with funding from NIH-NCI Cancer Center Support Grant P30 CA016059.

Acknowledgements

We thank Dr. Xianjun Fang's collaboration for mouse tissue for IHC, Drs. Jennifer Koblinski and Youngman Oh for their confirmation of histopathology interpretations, Drs. Daniel Conrad & Michael Maceyka for access to and use of laboratory equipment, Dr. Rebecca Martin for her insightful experimental discussions, and William Pearce for manuscript review and helpful suggestions.

Transparency document

Transparency document related to this article can be found online at https://doi.org/10.1016/j.bbrep.2019.100624.

Appendix A. Supplementary data

Supplementary data to this article can be found online at https://doi.org/10.1016/j.bbrep.2019.100624.

References

[1] F. Bray, et al., Global cancer statistics 2018: GLOBOCAN estimates of incidence and mortality worldwide for 36 cancers in 185 countries, Ca - Cancer J. Clin. 68 (6) (2018) 394–424.
[2] K.M. Fox, et al., Estimation of cachexia among cancer patients based on four definitions, J Oncol 2009 (2009) 693458.
[3] K. Fearon, et al., Definition and classification of cancer cachexia: an international consensus, Lancet Oncol. 12 (5) (2011) 489–495.
[4] J.M. Argiles, et al., Cancer cachexia: understanding the molecular basis, Nat. Rev. Canc. 14 (11) (2014) 754–762.
[5] J.A. Vaitkus, F.S. Celi, The role of adipose tissue in cancer-associated cachexia, Exp. Biol. Med. 242 (5) (2017) 473–481.
[6] N. Petrovic, et al., Chronic peroxisome proliferator-activated receptor gamma (PPARgamma) activation of epididymally derived white adipocyte cultures reveals a population of thermogenically competent, UCP1-containing adipocytes molecularly distinct from classic brown adipocytes, J. Biol. Chem. 285 (10) (2010) 7153–7164.
[7] J. Ishibashi, P. Seale, Medicine. Beige can be slimming, Science 328 (5982) (2010) 1113–1114.
[8] J. Nedergaard, T. Bengtsson, B. Cannon, Unexpected evidence for active brown adipose tissue in adult humans, Am. J. Physiol. Endocrinol. Metab. 293 (2) (2007) E444–E452.
[9] J. Gyamfi, et al., Multifaceted roles of interleukin-6 in adipocyte-breast cancer cell interaction, Transl Oncol 11 (2) (2018) 275–285.
[10] J.A. Carson, K.A. Baltgalvis, Interleukin 6 as a key regulator of muscle mass during cachexia, Exerc. Sport Sci. Rev. 38 (4) (2010) 168–176.
[11] T.A. Zimmers, M.L. Fishel, A. Bonetto, STAT3 in the systemic inflammation of cancer cachexia, Semin. Cell Dev. Biol. 54 (2016) 28–41.
[12] J. Lee, et al., Transition into inflammatory cancer-associated adipocytes in breast cancer microenvironment requires microRNA regulatory mechanism, PLoS One 12 (3) (2017) e0174126.
[13] J. Han, et al., Interleukin-6 induces fat loss in cancer cachexia by promoting white adipose tissue lipolysis and browning, Lipids Health Dis. 17 (1) (2018) 14.
[14] S. Kir, et al., Tumour-derived PTH-related protein triggers adipose tissue browning and cancer cachexia, Nature 513 (7516) (2014) 100–104.
[15] M. Petruzzelli, et al., A switch from white to brown fat increases energy expenditure in cancer-associated cachexia, Cell Metabol. 20 (3) (2014) 433–447.
[16] M. Tsoli, et al., Activation of thermogenesis in brown adipose tissue and dysregulated lipid metabolism associated with cancer cachexia in mice, Cancer Res. 72 (17) (2012) 4372–4382.
[17] U.L. Aune, L. Ruiz, S. Kajimura, Isolation and differentiation of stromal vascular cells to beige/brite cells, JoVE (73) (2013).
[18] J.C. Lownik, et al., ADAM10-Mediated ICOS ligand shedding on B cells is necessary for proper T cell ICOS regulation and T follicular helper responses, J. Immunol. 199 (7) (2017) 2305–2315.
[19] A. Ray, B.N. Dittel, Isolation of mouse peritoneal cavity cells, JoVE (35) (2010).
[20] J.C. Unkeless, Characterization of a monoclonal antibody directed against mouse macrophage and lymphocyte Fc receptors, J. Exp. Med. 150 (3) (1979) 580–596.
[21] R. Singh, et al., Increased expression of beige/Brown adipose markers from host and breast cancer cells influence xenograft formation in mice, Mol. Canc. Res. 14 (1) (2016) 78–92.
[22] B. Dirat, et al., Cancer-associated adipocytes exhibit an activated phenotype and contribute to breast cancer invasion, Cancer Res. 71 (7) (2011) 2455–2465.
[23] H. Green, M. Meuth, An established pre-adipose cell line and its differentiation in culture, Cell 3 (2) (1974) 127–133.
[24] B. Ni, et al., A novel role for PTK2B in cultured beige adipocyte differentiation, Biochem. Biophys. Res. Commun. 501 (4) (2018) 851–857.
[25] R.A. Garcia, J.N. Roemmich, K.J. Claycombe, Evaluation of markers of beige adipocytes in white adipose tissue of the mouse, Nutr. Metab. 13 (2016) 24.
[26] J. Wu, et al., Beige adipocytes are a distinct type of thermogenic fat cell in mouse and human, Cell 150 (2) (2012) 366–376.
[27] X. Liu, C. Cervantes, F. Liu, Common and distinct regulation of human and mouse brown and beige adipose tissues: a promising therapeutic target for obesity, Protein Cell 8 (6) (2017) 446–454.
[28] A. Ewens, E. Mihich, M.J. Ehrke, Distant metastasis from subcutaneously grown E0771 medullary breast adenocarcinoma, Anticancer Res. 25 (6B) (2005) 3905–3915.
[29] S.W. Perry, et al., Stromal matrix metalloprotease-13 knockout alters Collagen I structure at the tumor-host interface and increases lung metastasis of C57BL/6 syngeneic E0771 mammary tumor cells, BMC Canc. 13 (2013) 411.
[30] M. Battle, et al., Obesity induced a leptin-Notch signaling axis in breast cancer, Int. J. Cancer 134 (7) (2014) 1605–1616.
[31] E. Carrasco, et al., Meroxest improves the prognosis of immunocompetent C57BL/6 mice with allografts of E0771 mouse breast tumor cells, Arch. Med. Sci. 12 (5) (2016) 919–927.
[32] C.N. Johnstone, et al., Functional and molecular characterisation of EO771.LMB tumours, a new C57BL/6-mouse-derived model of spontaneously metastatic mammary cancer, Dis Model Mech 8 (3) (2015) 237–251.
[33] B.A. Pulaski, S. Ostrand-Rosenberg, Mouse 4T1 breast tumor model, Curr. Protoc. Im. 39 (1) (2001) 20.2.1–20.2.16 (Chapter 20): p. Unit 20 2.
[34] S. Yang, J.J. Zhang, X.Y. Huang, Mouse models for tumor metastasis, Methods Mol. Biol. 928 (2012) 221–228.
[35] F. Yang, et al., Inhibition of dipeptidyl peptidase-4 accelerates epithelial-mesenchymal transition and breast cancer metastasis via the CXCL12/CXCR4/mTOR axis, Cancer Res. 79 (4) (2018) 735–746.
[36] L.G. Martelotto, et al., Breast cancer intra-tumor heterogeneity, Breast Cancer Res. 16 (3) (2014) 210.
[37] G. Turashvili, E. Brogi, Tumor heterogeneity in breast cancer, Front. Med. 4 (2017) 227.
[38] R. Tanaka-Yachi, et al., Promoting effect of alpha-tocopherol on beige adipocyte differentiation in 3t3-L1 cells and rat white adipose tissue, J. Oleo Sci. 66 (2) (2017) 171–179.
[39] A. Yonezawa, et al., Boosting cancer immunotherapy with anti-cd137 antibody therapy, Clin. Cancer Res. 21 (14) (2015) 3113–3120.
[40] H.E. Kohrt, et al., Stimulation of natural killer cells with a CD137-specific antibody enhances trastuzumab efficacy in xenotransplant models of breast cancer, J. Clin. Investig. 122 (3) (2012) 1066–1075.
[41] T. Jarde, et al., Leptin and leptin receptor involvement in cancer development: a study on human primary breast carcinoma, Oncol. Rep. 19 (4) (2008) 905–911.
[42] L. Vona-Davis, D.P. Rose, Angiogenesis, adipokines and breast cancer, Cytokine Growth Factor Rev. 20 (3) (2009) 193–201.
[43] C.S. Cheng, Z. Wang, J. Chen, Targeting FASN in breast cancer and the discovery of promising inhibitors from natural products derived from traditional Chinese medicine, Evid Based Complement Alternat Med 2014 (2014) 232946.
[44] H. Fukuda, et al., Transcriptional regulation of fatty acid synthase gene by insulin/glucose, polyunsaturated fatty acid and leptin in hepatocytes and adipocytes in normal and genetically obese rats, Eur. J. Biochem. 260 (2) (1999) 505–511.
[45] D.K. Nomura, et al., Monoacylglycerol lipase regulates a fatty acid network that promotes cancer pathogenesis, Cell 140 (1) (2010) 49–61.
[46] Q. Chang, et al., The IL-6/JAK/Stat3 feed-forward loop drives tumorigenesis and metastasis, Neoplasia 15 (7) (2013) 848–862.
[47] F. Basolo, et al., Growth-stimulating activity of interleukin 6 on human mammary epithelial cells transfected with the int-2 gene, Cancer Res. 53 (13) (1993) 2957–2960.
[48] V. Mohamed-Ali, et al., Subcutaneous adipose tissue releases interleukin-6, but not tumor necrosis factor-alpha, in vivo, J. Clin. Endocrinol. Metab. 82 (12) (1997) 4196–4200.
[49] A. Sanguinetti, et al., Interleukin-6 and pro inflammatory status in the breast tumor microenvironment, World J. Surg. Oncol. 13 (2015) 129.
[50] F. Schaper, S. Rose-John, Interleukin-6: biology, signaling and strategies of blockade, Cytokine Growth Factor Rev. 26 (5) (2015) 475–487.
[51] E. Hagiwara, et al., Phenotype and frequency of cells secreting IL-2, IL-4, IL-6, IL-10, IFN and TNF-alpha in human peripheral blood, Cytokine 7 (8) (1995) 815–822.
[52] J.M. Harkins, et al., Expression of interleukin-6 is greater in preadipocytes than in adipocytes of 3T3-L1 cells and C57BL/6J and ob/ob mice, J. Nutr. 134 (10) (2004) 2673–2677.
[53] P.C. Heinrich, et al., Interleukin-6-type cytokine signalling through the gp130/Jak/STAT pathway, Biochem. J. 334 (Pt 2) (1998) 297–314.
[54] N. Schumacher, et al., Shedding of endogenous interleukin-6 receptor (IL-6R) is governed by A Disintegrin and metalloproteinase (ADAM) proteases while a full-length IL-6r isoform localizes to circulating microvesicles, J. Biol. Chem. 290 (43) (2015) 26059–26071.
[55] Y. Kuang, Z. Zhang, X. Zhang, [Interleukin-6 and its soluble receptors in human breast cancer], Zhonghua Zhongliu Zazhi 20 (4) (1998) 305–307.
[56] H.H. Oberg, et al., Differential expression of CD126 and CD130 mediates different STAT-3 phosphorylation in CD4+CD25- and CD25high regulatory T cells, Int. Immunol. 18 (4) (2006) 555–563.
[57] H. Ebsen, et al., Differential surface expression of ADAM10 and ADAM17 on human T lymphocytes and tumor cells, PLoS One 8 (10) (2013) e76853.
[58] L. Atapattu, et al., An activated form of ADAM10 is tumor selective and regulates cancer stem-like cells and tumor growth, J. Exp. Med. 213 (9) (2016) 1741–1757.
[59] J. White, IL-6, cancer and cachexia: metabolic dysfunction creates the perfect storm, Transl. Cancer Res. 6 (Supplement 2) (2017).